Int. J. Multiphase Flow Vol. 10, No. 6, pp. 663–676, 1984
Printed in the U.S.A.

0301–9322/84 $3.00 + .00
Pergamon/Elsevier

LARGE SCALE STRUCTURES IN GAS–LIQUID MIXTURE FLOWS

M. R. DAVIS
Department of Fluid Mechanics and Thermodynamics, University of New South Wales, Australia

and

B. FUNGTAMASAN
Faculty of Engineering, King Mongkut's Institute of Technology, Bangkok, Thailand

(*Received* 3 *May* 1983; *in revised form* 26 *January* 1984)

Abstract—Relatively slow variations in mixture void fraction in gas–liquid mixture flows are indicated by low pass filter averaging. The slow void fluctuations are found to have a regular characteristic frequency or scale in the churn flow regime or near the boundary with the dispersed bubble flow regime. These regular disturbances develop inherently in a vertical pipe flow in strength and in size and are not due to the method of flow mixing. There was no evidence of distinctive gas slugs in the flow, and the structures were identified as large clouds of bubbles which moved faster than the average velocity, growing in size and strength as they moved with the flow. The magnitude of the voidage fluctuations in the churn flow regime was on average 57% of the value for a slug flow. The large scale bubble clouds convect coherently over relatively long distances at up to 1.45 times the mean mixture flow velocity at a gas volume flow fraction of 0.4. In the bubble flow regime, the slow voidage variations were more random in scale and were only approx. 10% of the slug flow (maximum possible) value. However, even in the bubble flow regime, the disturbances convected coherently over relatively long distances at a velocity of approx. 1.1 times the mean mixture velocity.

1. INTRODUCTION

Gas–liquid mixture flows form a variety of complicated interfacial structures depending upon flow conditions. These range from relatively homogeneous, dispersed bubble forms to flows containing distinctive large slugs of the gas phase. At very low liquid fractions, liquid films form on flow boundaries and the central core of gas may contain fine liquid droplets or mist. There have been a number of classifications of flow regime based on visual observations, such as those of Vohr (1960), Hewitt (1976), Dukler & Taitel (1977) and Taitel (1980). In addition void sensitive probes have been used to determine mean conditions at points in the flow, such as void fraction and velocity (Delhaye 1969; Herringe & Davis 1974; Miller & Mitchie 1970; Jones & Delhaye 1976). In general intermittent flow effects have been related to the occurrence of large distinctive slugs of gas in the mixture (Griffith & Wallis 1961). However, visual observation of flows, particularly near the bubble/churn/slug condition boundaries, often suggests that a flow is not perfectly steady even if distinctive large slugs cannot be identified. It is the purpose of the present paper to describe experiments directed towards quantitative identification of intermittent flow effects under bubbly or churn conditions for which distinctive large slugs were not observable.

Observations in the present experiments were made under generally similar conditions of flow in the same apparatus used by Herringe & Davis (1976, figure 1). The flows used in the present work were chosen to lie in the vicinity of the transition between bubble and churn flows, as discussed by Taitel *et al.* (1980) for example. Figure 2 shows the location of the flows used on the flow regime map of Taitel *et al.* based on the superficial velocities of gas and liquid phases (air and water in these experiments). The superficial velocity is obtained by dividing the volumetric flow rate for a phase by the total flow cross sectional area. The experiments have been carried out in the dispersed bubble and churn flow regime, and the superficial velocities in the present experiments have been carefully selected to lie to either side of this boundary as shown in figure 2. The flow conditions are also shown in table 1. The

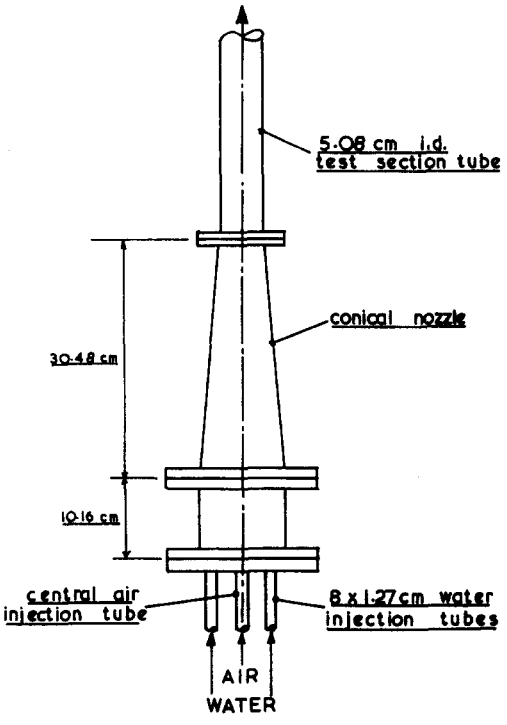

Figure 1. General arrangement of test apparatus used in the experiments.

average mixture velocity (U_m) is the sum of the superficial velocities of the two phases, and is equal to the ratio of total volumetric flow rate to cross sectional area.

Throughout this paper it is necessary to distinguish clearly between the rapidly fluctuating instantaneous phase (gas or liquid sensed by a point needle probe) and the fluction in void fraction as discussed in section 2. The latter is a relatively slow variation average gas content occurring at a rate of order 100 times slower than the former. It is also necessary to distinguish between volume flow fraction (β, the ratio of total gas phase volumetric flow to total volumetric flow) and mean local void fraction ($\bar{\alpha}$ at a point, the fraction of total time the gas phase is present at the point). Due to the distribution of mean local void fraction ($\bar{\alpha}$) over the flow cross section as discussed by Herringe & Davis (1976) and due to relative motion between the phases, the area average of the void fraction is not generally equal to β, and point values of $\bar{\alpha}$ may differ significantly from β.

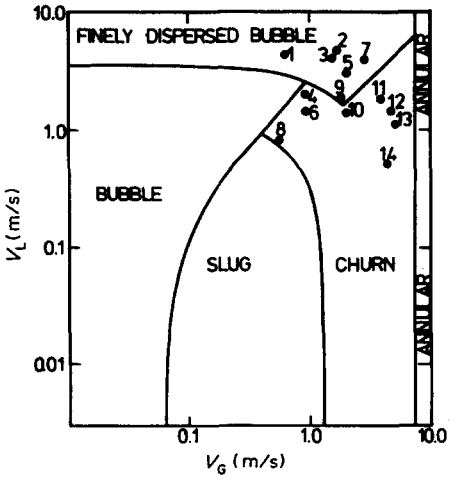

Figure 2. Location of flows investigated on the flow regime map of Taitel *et al.* (1980).

Table 1. Magnitude of fluctuations (at flow centre line)

Flow Cond.	U_m m/s	β	Lower - Probe (0.65 m above mixer)					Upper - Probe (2.71 m above mixer)				
			$\bar{\alpha}$	τ_c (sec)	W_ω (sec^{-2})	α_{rms}	$\frac{\alpha_{rms}}{\bar{\alpha}}$	$\bar{\alpha}$	τ_c (sec)	W_ω (sec^{-2})	α_{rms}	$\frac{\alpha_{rms}}{\bar{\alpha}}$
1	5.17	0.12	.125	2.5	36.2	0.085	0.68	.100	2.5	51.1	0.036	0.36
2	6.52	0.25	.300	2.5	36.9	0.138	0.46	.258	2.5	41.2	0.049	0.19
3	5.72	0.26	.300	2.5	30.1	0.138	0.46	.270	2.5	43.3	0.067	0.23
4	3.03	0.30	.525	2.5	56.7	0.356	0.68	.520	2.5	68.3	0.249	0.48
5	5.18	0.38	.663	2.5	38.6	0.293	0.44	.615	2.5	86.5	0.240	0.39
6	2.41	0.38	.506	10.0	35.9	0.360	0.71	.493	10.0	16.1	0.320	0.65
7	6.96	0.39	.625	2.5	53.8	0.218	0.35	.616	2.5	96.5	0.132	0.30
8	1.42	0.40	.475	10.0	21.8	0.373	0.79	.435	10.0	12.0	0.329	0.76
9	3.74	0.48	.713	10.0	42.9	0.285	0.40	.686	10.0	25.8	0.285	0.42
10	3.46	0.57	.750	10.0	26.2	0.271	0.36	.718	10.0	17.0	0.276	0.39
11	5.84	0.67	.875	10.0	18.8	0.120	0.14	.850	10.0	20.2	0.209	0.25
12	6.10	0.76	.925	10.0	10.6	0.080	0.09	.902	10.0	12.7	0.124	0.19
13	6.34	0.81	.938	10.0	11.3	0.084	0.09	.938	10.0	9.13	0.156	0.17
14	4.89	0.89	.981	10.0	8.92	0.054	0.06	.957	10.0	6.48	0.138	0.15

2. OBSERVATION OF UNSTEADY VARIATIONS OF VOID

Experiments were carried out in a flow of an air water mixture using needle probe sensors to detect instantaneous changes in the phase present at the probe as described by Herringe & Davis (1974, 1976). These probes are made from very sharp surgical needles of stainless steel, and have been shown to resolve bubbles reliably down to a size of 0.1 mm. The probes are constructed from needles selected under a microscope to have the sharpest tip, with a radius of order 0.01 mm. Subsequently the needle is coated with epoxy which is allowed to run back from the tip under gravity whilst drying to expose only the tip area to contact with the flow. Probes are finally selected on the basis of the smallness of bubble which can be sensed, as indicated by the time for the bubble to pass the probe, and it is found that 0.1 mm represents the best resolution which could be achieved (Herringe & Davis 1974, 1976). The probes are operated in a Wheatstone bridge circuit with an 80 KHz alternating voltage excitation, the bridge being balanced to give zero output in the liquid phase. The modulated 80 KHz output which results from bridge unbalance in the air phase is used to activate a demodulator and gate circuit to produce a two stage voltage signal representing the phase instantaneously present at the probe tip (e.g. as shown in figure 4a). Davis & Herringe (1974) have verified the accuracy of this sensing system, by integrating gas volume flux from void fraction (fraction of time in gas phase) and velocity (sensed by two needle cross correlation) data integrated over the flow cross section which agreed with injected flow rate to approx. 3%.

The two state signal from the probe amplifier system can be time averaged to give the flow void fraction by passing it through a resistor–capacitor (resistance R, capacitance C) low pass filter output network. The void fraction (α) is defined as the fraction of time the gas phase is present at the sensing position. By selecting the time constant of this network appropriately, the output will also show relatively slow variations in the void fraction at the sensing point and hence can be used to provide an indication of unsteadiness in the flow. In the following paragraphs the response of this single time constant averager to fluctations in void fraction which are very slow relative to individual bubble durations at the sensing point will be discussed.

Figure 3 illustrates the response of the averaging network; provided that the time of individual bubble and liquid elements at the probe is relatively short compared with the time constant ($\tau_c = CR$) of the averager, each section of the averager output may be approximated by a ramp function in place of the exponential function of which the ramp

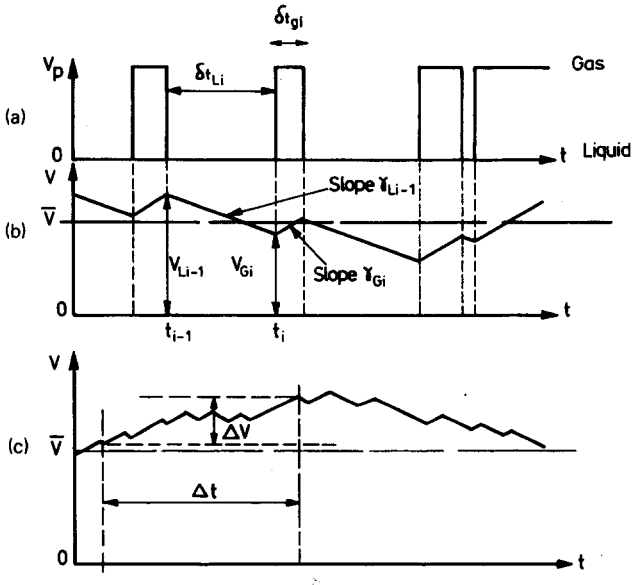

Figure 3. (a) Two state signal from needle probe representing gas or liquid phase at probe. (b) Low pass average signal, average void fraction = $\bar{V}/V_p$. (c) Long period changes in the averaged signal.

forms the first part only. The slopes (γ_G, γ_L) of the ramps are (see figure 3 for notation):

$$\gamma_{Gi} = \frac{V_p - V_{Li-1}}{\tau_c}$$

on rising sections when the probe is in the gas phase, and:

$$\gamma_{Li} = \frac{V_{Gi}}{\tau_c}$$

on falling sections when the probe is immersed in the liquid phase. V_p is the output voltage from the probe when it is in air, there being a zero output when in the liquid phase. Provided that the time constant is sufficiently large, variations in the output voltage from the overall average value $\bar{V}$ will be small and we may replace V_{Gi} and V_{Li-1} in these expressions by $\bar{V}$. Thus we have:

$$\frac{\gamma_G}{\gamma_L} = \frac{\gamma_{Gi}}{\gamma_{Li}} = -\frac{V_p - \bar{V}}{\bar{V}} = -\frac{1-\bar{\alpha}}{\bar{\alpha}} \qquad [1]$$

where the mean void fraction is $\bar{\alpha} = \dfrac{\bar{V}}{V_p}$.

The variation of the output voltage ΔV over a time interval Δt can be written as:

$$\Delta V = \sum_{\Delta t} (\gamma_G \delta t_{Gi} + \gamma_L \delta t_{Li}) \qquad [2]$$

where δt_{Gi} and δt_{Li} are the time durations of individual gas or liquid elements at the probe (δt_{Gi}, $\delta t_{Li} \ll \Delta t$, so that we are considering variations in ΔV which take place over times which are long compared with the duration of each gas or liquid element at the probe). We may rearrange this in the form:

$$\frac{\Delta V}{\Delta t} = \frac{\gamma_G \Sigma \delta t_{Gi}}{\Sigma \delta t_{Gi} + \Sigma \delta t_{Li}} \left\{ 1 + \frac{\gamma_L \Sigma \delta t_{Li}}{\gamma_G \Sigma \delta t_{Gi}} \right\}. \qquad [3]$$

If the void fraction in the flow fluctuates about the mean value $\bar{\alpha}$ by an amount α , then the void fraction is:

$$\alpha = \bar{\alpha} + \alpha' = \frac{\Sigma \delta t_{Gi}}{\Sigma \delta t_{Gi} + \Sigma \delta t_{Li}}. \qquad [4]$$

Thus on substituting we have, replacing $\Delta V/\Delta t$ by $\mathrm{d}V/\mathrm{d}t$:

$$\frac{\mathrm{d}V}{\mathrm{d}t} = \gamma_G \alpha \left(1 + \frac{\gamma_L}{\gamma_G} \frac{1-\alpha}{\alpha}\right) = \gamma_G \alpha \left(1 - \left(\frac{\bar{\alpha}}{1-\bar{\alpha}}\right)\left(\frac{1-\alpha}{\alpha}\right)\right).$$

Thus we have:

$$\frac{\mathrm{d}V}{\mathrm{d}t} = \frac{\gamma_G(\alpha - \bar{\alpha})}{1-\bar{\alpha}} = \frac{\gamma_G \alpha'}{1-\bar{\alpha}} = \frac{V_p}{\tau_c} \alpha'. \qquad [5]$$

We see that if the relatively slow (compared with the individual void element times) fluctuations in voidage are α' about the overall average $\bar{\alpha}$, then the output of the low pass filter averager increases in proportion to α'. The influence of the time constant of the filter

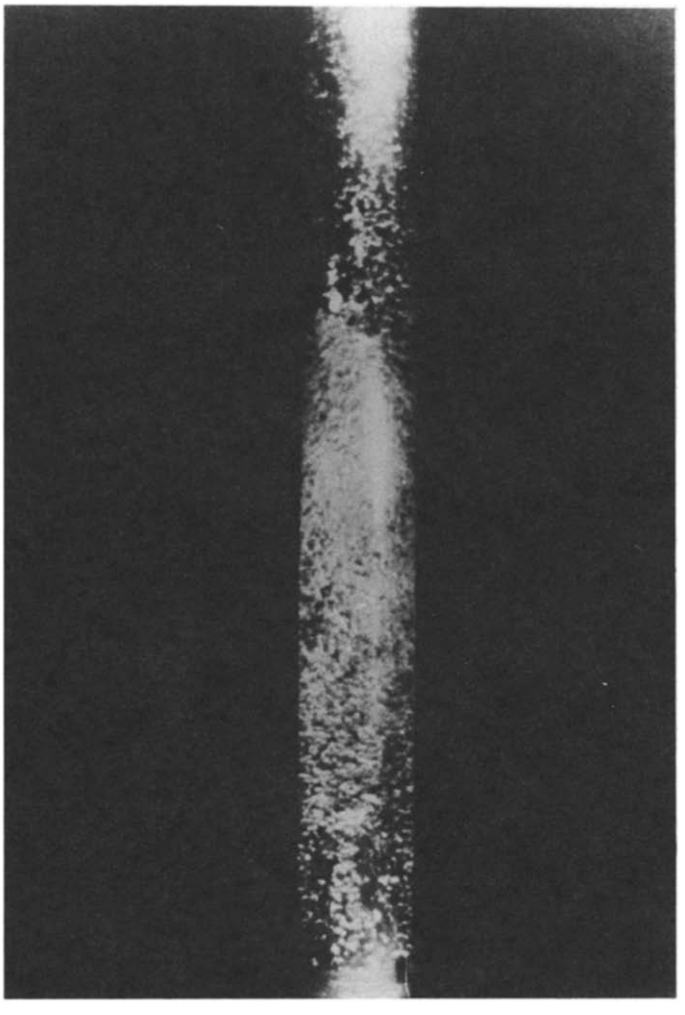

Figure 4. Instantaneous photograph showing a developing concentration or cloud of bubbles (flow 8).

$\tau_c = RC$ is to scale the magnitude of the output voltage fluctuations, but variations in τ_c will not influence the temporal form of these variations (ΔV).

The experimental results were obtained in a vertically upwards flow of an air–water mixture in a 5.08 cm dia. circular pipe. The two phases were mixed in a conical chamber leading into the pipe, air being injected at the centre and water through a set of holes around the air injector hole in the base of the chamber. The flow from this mixer has been described in detail by Herringe & Davis (1976), and has been found to adopt mean distributions of voidage and velocity characteristic of vertical flow more rapidly than other mixing devices. The conical chamber was 32 cm long with a base diameter of 9 cm. As shown in figure 2 the flow rates of air and water were selected to lie around the bubble/churn flow transition, and visual observation of the flow showed it to be somewhat unsteady, with intermittent concentrations of gas developing as the flow moved vertically at a few cycles per second depending upon flow conditions. High speed motion film (at 2000 frames per second) and flash photographs (e.g. see figure 4) suggested that the intermittency was due to the formation of concentrations or clouds of bubbles. Distinctive large slugs were not observed either visually or from the output traces of the needle probe (figure 5a). Whilst it was thus possible to observe the intermittent formation of what appeared to be concentrated bubble clouds, and to observe their motion with the flow, such visual observations cannot provide a detailed quantitative record of the flow structure, and so the single time constant averaging network described in the foregoing discussion was introduced to the needle probe output signal.

The operation of a void detection probe with a low pass averaging filter as described is illustrated in figure 5 which shows typical waveforms of the acutal void probe itself and

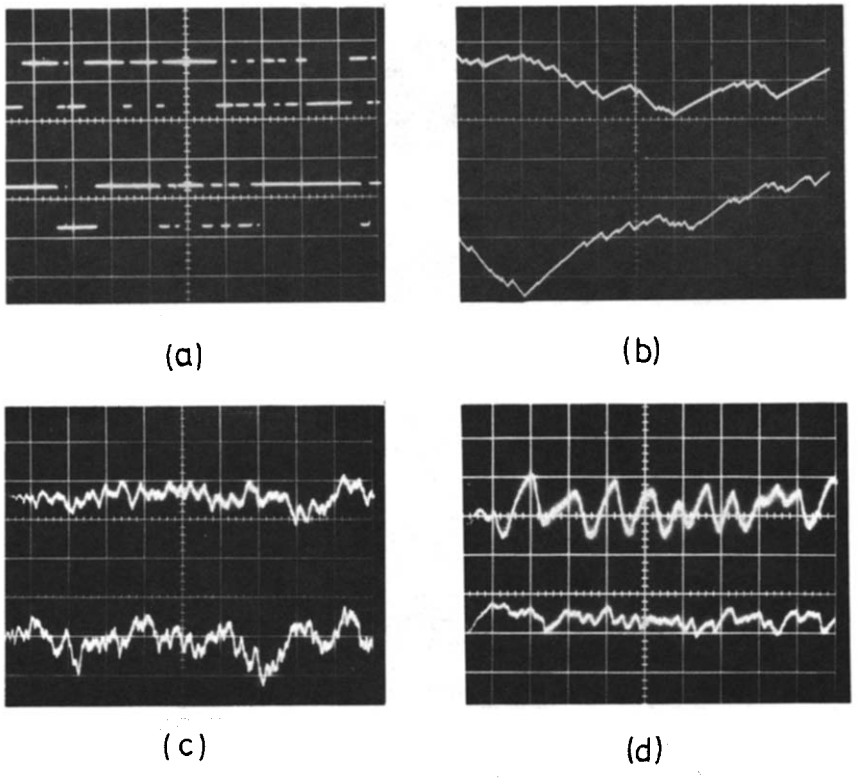

Figure 5. Unsteady voidage signals for upwards pipe flow at pipe centre line. (a) Two state probe signal-up denotes air, down denotes water (2 ms/cm, 2 V/cm). (b) Short term averaged void signal showing slow void fluctuations (2.5 s time constant) 5 m/s/cm, 0.1 V/cm, gain = 20. (c) and (d) As (b), 0.2 s/cm, 0.5 V/cm. Lower trace—lower probe 0.65 m above mixer; upper trace—upper probe 2.71 m above mixer. (a), (b) and (c) U_m = 4.9 m/s, β = 0.38; (d) U_m = 5.9 m/s, β = 0.67. Pipe dia. = 5.08 cm.

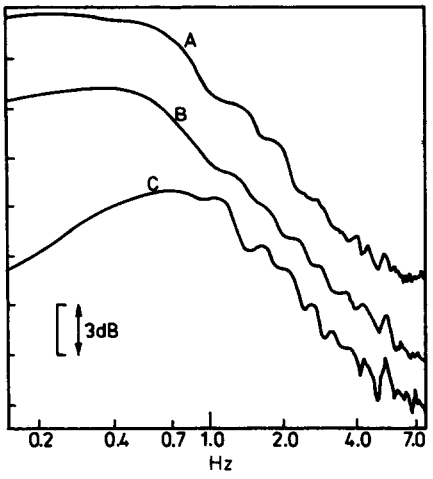

Figure 6. Influence of averager time constant on spectrum of void fluctuation signal at centre line (upward bubble flow, 5.9 m/s, $\beta = 0.39$). Curve A: $\tau_c = 10$ s; B; $\tau_c = 2.5$ s; C: $\tau_c = 0.25$ s.

of the averager output. The latter shows clearly that the flow contains relatively slow fluctions in voidage about the mean value. To check the validity of the preceding discussion, variations were made in the time constant τ_c, and it was found that the magnitude of the output decreased as expected in inverse proportion to τ_c. Figure 6 shows frequency spectra of the low pass filter output with different time constants. For the two longer time constants the spectra are similar in shape, confirming that these values (i.e. $\tau_c = 10$ s, 2.5 s) are sufficiently long to ensure that the output voltage represents the voidage fluctuation in the form given in [5]. However, for the smallest value of τ_c shown in figure 6 ($\tau_c = 0.25$ s) we see that there has been a significant decrease in the low frequency components of the spectrum. It is concluded that this time constant is too short for observation of the voidage fluctuation in this particular flow. Attenuation of very low frequency components in this manner is associated with the occurrence of relatively large fluctuations in output about $\bar{V}$, so that values approaching zero or V_p can be observed in the signals with corresponding reductions in the slopes of the signal ramps γ_{Gi} and γ_{Li} for individual void or liquid elements.

Equation [5] shows that the rate of change of the averaging filter output voltage, dV/dt, is proportional to the perturbation of the void fraction. It follows that the power spectra of the output voltage $\phi_v(\omega)$ and of the void fraction $\phi_\alpha(\omega)$ are related by:

$$\phi_\alpha(\omega) = \left(\frac{\tau_c}{V_p}\right)^2 \omega^2 \phi_v(\omega) \qquad [6]$$

where ω is the angular frequency parameter. It also follows that the mean square fluctuations $\overline{V'^2}$ and $\overline{\alpha'^2}$ are related by:

$$\overline{\alpha'^2} = \left(\frac{\tau_c}{V_p}\right)^2 W_\omega \overline{V'^2} \qquad [7]$$

where W_ω depends upon the form of the frequency spectra and is given by:

$$W_\omega = \frac{\int_0^\infty \omega^2 \phi_v(\omega)\, d\omega}{\int_0^\infty \phi_v(\omega)\, d\omega}. \qquad [8]$$

Figure 7 shows an example of the conversion of the observed voltage fluctuation spectrum into the void fluctuation spectrum, the former being observed by passing the voltage signal from the averaging filter to a Hewlett–Packard 3582A analyser. It should be noted that the dominant contribution to the unsteady voidage occurs at approx. 7 Hz, and that fluctuation components above 40 Hz are almost neglible. In contrast, individual bubbles have a typical passage frequency (e.g. see figure 4a) of over 500 Hz. Thus we see that it is reasonable to represent the voidage fluctuations as being relatively slow compared with individual void durations as the above analysis has assumed.

Whilst individual bubbles undergo relatively rapid deformation and rearrangement within a turbulent two phase pipe flow, the relatively slow variations in void fraction retain their identity over much longer times. The cross correlation function between two void probe instantaneous bubble signals was found by Herringe & Davis (1976) to decay over a relatively short distance of several centimeters, and the passage of flow disturbances over longer distances cound not be observed. In contrast, the transport of slow fluctuations in void fraction was found to be observable over much longer distances, as shown in figure 8a. The correlation between signals is quite clear over a distance of 2.06 m, and when transformed into the frequency domain to obtain the phase spectrum, the resulting phase velocity is well defined (figure 8b). These results show that an application of the averaging filter method introduced here is to the observation of the propagation of large disturbances through complete flow systems and could thus have a useful application in the study of overall system dynamics. Identification of convective motion over relatively long distances did not depend upon the void fluctuations possessing a distinctive large scale, since the correlation existed whether or not their frequency spectrum showed a characteristic peak. Thus flows which did not have a characteristic scale for the voidage fluctuations did contain significant fluctuations of voidage of a more random nature, and these random fluctuations propagated with the flow in a similar manner to the propagation of the distinctive scale disturbances observed in the churn flow regime. As figure 8 shows, the void fraction perturbations move at approx. 1.45 times the average mixture velocity (U_m, the sum of the superficial velocities of the two phases). At lower gas volume flow fractions ($\beta < 0.3$, where β = gas phase volumetric flow rate/total volumetric flow rate), it was found that the void fluctuations moved at velocity much closer to the average mixture velocity (e.g. at about 1.1 times the average mixture velocity) and it appears that in general higher velocities of the voidage disturbances occur in the churn flow regime than in the bubble flow regime.

The phase velocities for the bubble clouds exceed both the average gas and liquid phase velocities, and are thus in excess of the voidage wave velocities observed by Bouré & Mercadier (1982). However, their experiments were at relatively low void fractions and

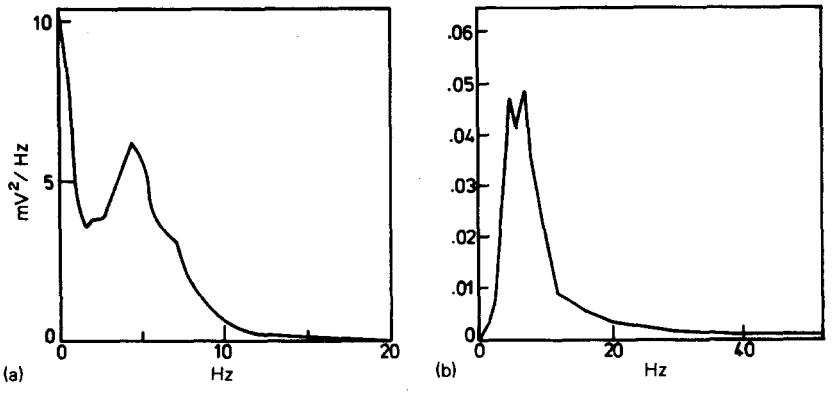

Figure 7. (a) Spectral density of averager output voltage. (b) Spectral density of voidage fluctuations from (6) (churn flow in a vertical pipe, at centre line, flow 9).

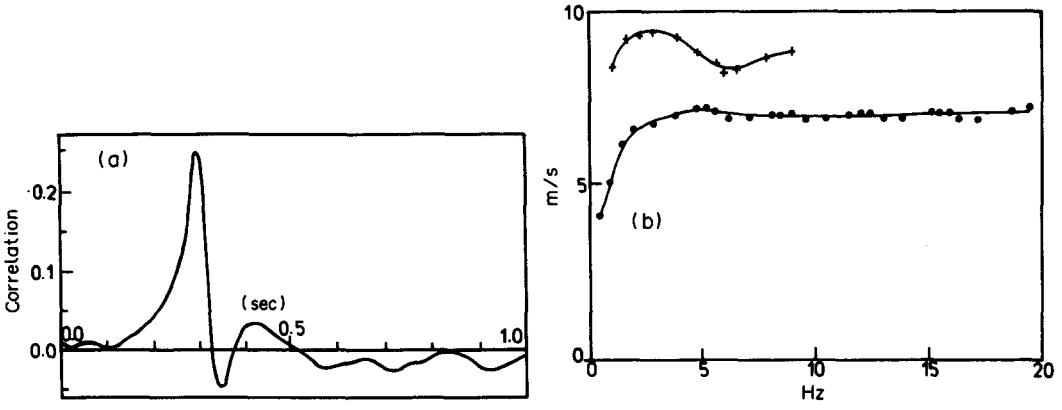

Figure 8. (a) Cross-correlation between low pass averaged void signals of two probes on the centre line separated by a distance of 2.06 m in a 5.08 cm vertical pipe (lower probe is 0.65 m above mixer, $U_m = 4.9$ m/s, $\beta = 0.38$). (b) Phase velocity obtained by transformation of (a) (⊙: $U_m = 4.9$ m/s, $\beta = 0.38$; +: $U_m = 5.9$ m/s, $\beta = 0.67$).

velocities and lay on the bubble/slug transition boundary rather than the bubble/churn transition boundary. It appears, therefore, that the mechanism responsible for the void fraction wave in Bouré and Mercadier's observations is distinct from the bubble cloud phenomenon observed here. The former gives rise to a velocity intermediate between mean gas and liquid velocity, whilst the latter gives rise to a disturbance propagating faster than these mean velocities.

3. DEVELOPMENT OF LARGE SCALE VOIDAGE VARIATIONS

The results of section 2 showed that the voidage fluctuations near the churn/bubble transition were concentrated over a relatively small range of low frequency, and that they propaged at a velocity in excess of the average mixture velocity. In this section we will examine the development of these flow disturbances in vertical pipe flows in more detail.

As described by Herringe & Davis (1976), the flow was mixed in a conical mixing chamber at the entry to the vertical 50 mm dia. pipe. In order to determine that the observed disturbances were inherent to the flow and not introduced by the mixing

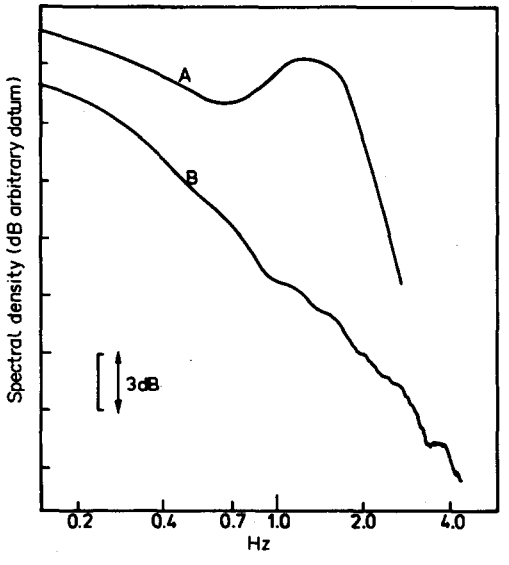

Figure 9. Development of distinctive disturbances in vertical pipe flow (flow 8 at centre line). Curve A: spectrum of low pass average 2.71 m above flow mixer; curve B: spectrum 0.65 m above flow mixer.

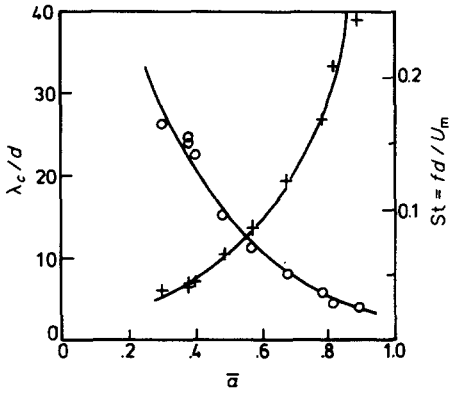

Figure 10. Variation of characteristic Strouhal number and length scale with mean local void fraction $\bar{\alpha}$ in the churn flow regime. ○ Strouhal number, right hand scale; + λ_c/d left hand scale (observed at centre line, 2.71 m above mixer).

chamber, observations were made at distances of 0.65 m and 2.71 m above the exit from the mixer. Figure 9 shows spectra of the fluctuations observed at the two positions, and it is clear that the distinctive fluctuations at several cycles per second in this case were not present near to the mixing chamber, but had developed quite strongly at the second observation position. Similar effects were observed for most of the flows shown in figure 2, with the exception of flows 1, 2 and 3 where the spectra did not develop a distinctive peak at all. Also, flows 4, 5 and 7 did not show quite such a sharply defined peak developing. Thus we see that in the finely dispersed bubble flow regime of Taitel *et al.* (figure 2) the voidage fluctuations, whilst still present and still displaying convection over long distances, do not suggest any regular large scale patterns. However, as the churn flow boundary is approached and in the churn flow regime itself, there is evidence of a more regular pattern of voidage non–uniformity developing within the flow after leaving the mixing chamber.

Where a distinct peak in the frequency spectrum of voidage fluctuations occurred it was found that this varied in a systematic manner with the mean local void fraction ($\bar{\alpha}$). This is shown in figure 10 in terms of the Strouhal number (St) based on average mixture velocity (U_m). If the disturbances are represented by a characteristic length ($\lambda_c = U_m/f_c$, where f_c is the characteristic frequency), we see that this increases progressively from approx. 5 tube diameters at low gas content ($\bar{\alpha} = 0.25$) to 35 dia. at high gas content ($\bar{\alpha} = 0.8$). Furthermore, as figure 11 shows that there was a regular tendency for this characteristic length to increase as the disturbances moved with the flow. It was not found

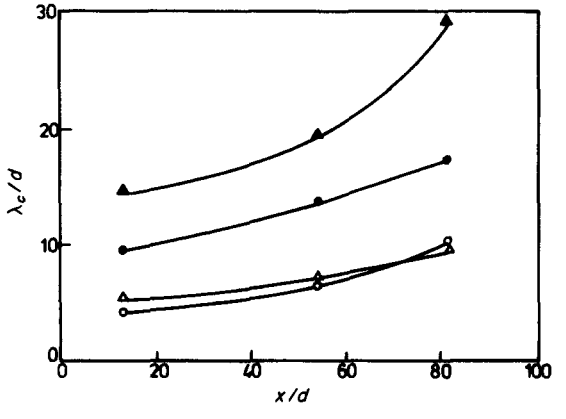

Figure 11. Increase of scale disturbances along the flow; ○ flow 5; △ flow 8; ●; flow 10; ▲; flow 11 (observed at centre line).

that there was any systematic variation of the scale of the disturbances with mixture velocity.

The magnitude of the voidage fluctuations ($\overline{\alpha'^2}$) can be determined from the averaging filter output (V') by [7], provided that the averager time constant (τ_c) and amplitude of the two state pulse signal representing instantaneous phase variations (V_p) are known. It is also necessary to know the frequency spectrum $\phi(\omega)$ so that the weighting factor W_ω can be determined form [8]. The results for the various flow conditions are given in table 1, and the relative root mean square to mean voidage ratio ($\sqrt{\overline{\alpha'^2}}/\bar{\alpha}$) is shown in figure 12 as a function of local mean void fraction $\bar{\alpha}$. This ratio has a maximim possible value for a slug flow, where the void fraction changes between the values of zero and unity at a relatively slow rate. Analysis of the fluctuating voidage signals shows that for a slug flow:

$$\left[\frac{\sqrt{\alpha'^2}}{\bar{\alpha}}\right]_{max} = \sqrt{1/\bar{\alpha} - 1}. \qquad [9]$$

This maximum limit is also plotted on figure 12, and it is seen that the values observed are substantially below the maximum value. The flow conditions 1,2 and 3 give results with the lowest fluctuation relative to the maximum (between 11 and 30%), reflecting the more homogeneous nature of these flows in the bubble regime (figure 2). For these flows the void fluctuation decreases significantly in the flow direction. For the remaining flows, near to the churn/bubble boundary or in the churn flow region, the void fluctuations are relatively larger at 57% of the maximum limiting value on average over all the results. Close to the churn/bubble boundary the fluctuations did not vary significantly along the flow, but further into the churn flow regime the fluctuations in voidage increased quite strongly in the flow direction.

The voidage fluctuations were found to be largest at a local mean void fraction $\bar{\alpha} \simeq 0.45$, as shown in figure 13. Examination of the results in detail (table 1) also shows a trend for the fluctuations to be stronger at lower average flow velocities. In view of the relatively small number of data points available it is not possible to propose any precise

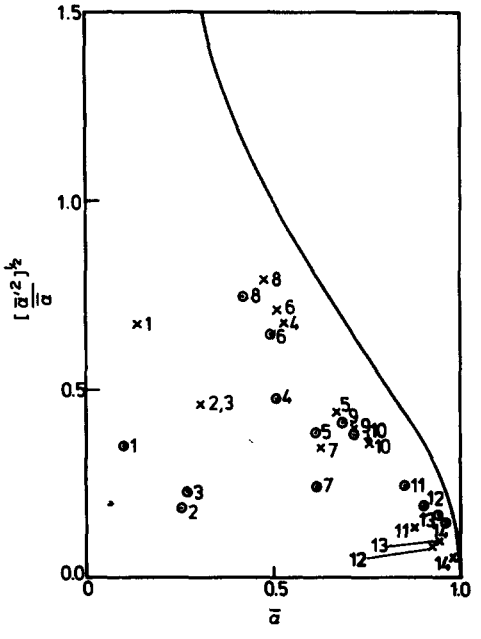

Figure 12. Ratio of void fluctuation magnitude at centre line to maximum value for slug flow. Solid line; maximum limit, [9]; points; x; 0.65 m above mixer; ⊙; 2.71 m above mixer. Numbers denote flow condition (figure 1 and table 1).

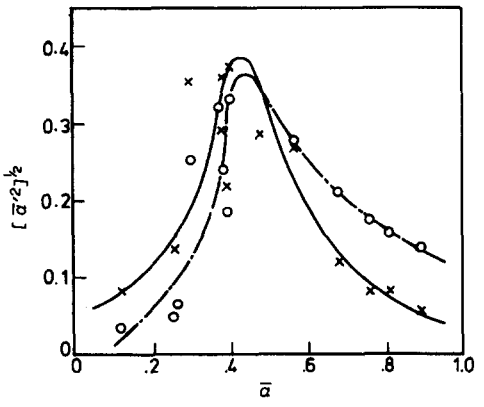

Figure 13. Variation of void fluctuation magnitude with mean local void fraction (notation as figure 11).

relationship between the mean flow speed and volume flow fraction and the levels of voidage fluctuation.

4. CONCLUSION

It has been found that gas liquid mixture flows contain relatively slow variations in local voidage in the dispersed bubble and churn flow modes. The disturbances retained their identity over relatively long distances along the flow direction, showing clear corrleation functions from which their velocity of convection could be clearly identified. In the churn flow regime and near to the churn/bubble regime boundary these long term variations have a distinctive frequency, corresponding to disturbances with an axial length scale between 5 and 40 tube diameters in vertical, upward pipe flow. These regular disturbances were not introduced by the flow mixer at inlet, but rather developed progressively with an increase of scale and strength as the flow moved along the pipe. Distinctive large gas slugs could not be observed, and the disturbances were thus identified as intermittent clouds or concentrations of bubbles. The velocity of these clouds exceeded the mean flow velocity. It thus appears that the mechanism for development of a bubble cloud is one by which a perturbation in void fraction moves through the mixture, entraining bubbles from the region in front of the disturbance and increasing in magnitude and scale.

The magnitude of the variations in void fraction was larger in the churn flow regime than in the dispersed bubble regime, and in the churn flow regime was about 57% of the maximum value which would apply for a simple slug flow. For no condiditon of flow was a void fluctuation in excess of 75% of the maximum value observed. The voidage fluctuations were strongest at a mean local void fraction of 0.45 approx., and were also stronger at lower mean flow velocities. The fluctuations showed a strong tendency to increase along the flow for conditions furthest from the bubble/churn boundary in the churn flow regime. For flows in the bubble flow regime, slow variations of void fraction with a magnitude of approx. 10% of the maximum for slug flow were observed. These bubble regime void fluctuations also convected coherently over relatively long distances, but did not show a particular characteristic scale. Thus the void fluctuatoins in the bubble flow regime are seen to be more randomly variable in their scale.

Whilst the observations discussed here have been made in vertical flow, visual observations of the flow in the same test rig when oriented horizontally suggest that similar conditions of progressive development of bubble clouds occur in horizontal flows. In both cases the tests suggested that the flow was undergoing a progressive development not induced at the inlet by the mixer and within the length of the test rig it did not appear

that the disturbances had reached a steady state at large distances from the mixer. As discussed by Davis (1974) the mean flow undergoes significant acceleration due to the frictional pressure drop, thus precluding attainment of a flow structure independent of position along the pipe as is the case for incompressible flows.

REFERENCES

BOURÉ, J. A. & MERCADIER, Y. 1982 Existence and properties of flow structure waves in two phase bubbly flows. *Appl. Sci. Res.*, **38**, 297–303.

DAVIS, M. R. 1974 Determination of wall friction in vertical and horizontal two phase flow. *ASME J. Fluids Engng* **96**, 173–197.

DELHAYE, J. M. 1969 Hot film anemometry in two phase flow. 11*th Nati. ASME/AIChE Heat Transfer Conf.*, Minneapolis,.

DUKLER, A. E. & TAITEL, Y. 1977 Flow regime transitions for vertical upward gas liquid flow'. *Progress Report No.* 1, *NUREG*–0162, *NCR* 2.4. Nuclear Regulatory Commission.

GRIFFITH, P. and WALLIS, G. B. 1961 Two phase slug flow. *ASME J. Heat Transfer* **83C**, 307–320.

HERRINGE, R. A. & DAVIS M. R. 1974 Detection of instantaneous phase changes in gas–liquid mixture. *J. Phys. E., Sci. Instruments* **7**, 807–812.

HERRINGE, R. A. & DAVIS M. R. 1976 Structural development of gas–liquid mixture flows. *J. Fluid Mech.* **23**, 97–123.

HEWITT, G. F. 1976 *Two phase Flow Patterns and Their Relationship to Two Phase Heat Transfer.* NATO Advanced Study Institute, Istanbul. Hemisphere, Washington.

JONES, O. C. & DELHAYE, J. M. 1976 Transient and statistical measurement techniques for two phase flows: a critical review. *Int. J. Multiphase Flow* **3**, 89–116.

GOLAN, L. P. & STENNING, A. H. 1969 Two phase vertical flow maps. *Proc. Inst. Mech. Engrs* **184**, 108 000.

MILLER, N. & MITCHIE, R. E. 1970 Measurement of local voidage in gas liquid two phase flow systems, a universal probe. *J. Br. Nucl. Engng Soc.* **9**, 94–100.

TAITEL, Y., BARNEA, D. & DUKLER, A. E. 1980 Modelling of flow pattern transition for steady upward gas liquid flow in vertical tubes. *AIChE J.* **26**.

VOHR, J. H. 1960 Flow patterns of two phase flow—a survey. *TID*–11514. U.S. Atomic Energy Commission.